

Sandwich: Separating Prefill-Decode Compilation for Efficient CPU LLM Serving

Juntao Zhao[†]

The University of Hong Kong
Hong Kong, China
jtzhao@connect.hku.hk

Jiuru Li[†]

The University of Hong Kong
Hong Kong, China
u3011183@connect.hku.hk

Chuan Wu

The University of Hong Kong
Hong Kong, China
cwu@cs.hku.hk

Abstract

Utilizing CPUs to serve large language models (LLMs) is a resource-friendly alternative to GPU serving. Existing CPU-based solutions ignore workload differences between the prefill and the decode phases of LLM inference, applying a static per-NUMA (Non-Uniform Memory Access) node model partition and utilizing vendor libraries for operator-level execution, which is suboptimal. We propose Sandwich, a hardware-centric CPU-based LLM serving engine that uses different execution plans for the prefill and decode phases and optimizes them separately.

We evaluate Sandwich across diverse baselines and datasets on five CPU platforms, including x86 with AVX-2 and AVX-512, as well as ARM with NEON. Sandwich achieves an average 2.01× throughput improvement and 90% satisfactory time-to-first-token (TTFT) and time-per-output-token (TPOT) latencies with up to 3.40× lower requirements in single sequence serving, and significant improvement in Goodput in continuous-batching serving. The GEMM kernels generated by Sandwich outperform representative vendor kernels and other dynamic shape solutions, achieving performance comparable to static compilers with three orders of magnitude less kernel tuning costs.

1 Introduction

Large language models (LLMs) have unlocked a broad spectrum of AI-driven applications [43]. Since the LLM serving workload involves computational-demanding general matrix multiplications (GEMM), recent LLM serving solutions have favored GPUs over CPUs because of GPUs’ larger parallel-computing capability. Such solutions include memory management and parallelism serving strategies as in vLLM [35] and Liger [13], kernel optimization like FlashAttention [10] and RingAttention [36], and vendor solutions or open-source serving platforms including FastTransformer [40], TurboTransformer [15] and DeepSpeed Inference [2].

Research attentions are attracted to the largely underexplored potential for CPU-based LLM inference. High-caliber GPUs are often in shortage [62], whereas CPUs are more available and typically underutilized in AI clusters. Hu [24] reported that less than 25% CPUs are used in 75% tasks, compared to much higher utilization of GPUs, in two LLM training clusters (Seren and Kalos). Leveraging idle CPUs for LLM computation provides substantial cost savings while being able to meet application service level objectives (SLOs). For example, a TPOT (time per output token) of 280ms (which is close to human reading speed (250ms) [67]) can be achieved for single sequence inference over an FP32 Llama-1.3b model on

two Intel(R) Xeon(R) CPU E5-2630 processors (purchase cost at USD 242.70). Existing CPU-based LLM-serving solutions such as the CPU backend of vLLM [35], llama.cpp [20], and xFasterTransformer [26] commonly port GPU-based methods and execution plans directly to CPU environments. Ongoing research on CPU serving predominantly focuses on quantization techniques, exemplified by approaches proposed by Intel [50] and the Lookup Table from NoMAD-Attentions [61]. There are also efforts made toward serving Transformer models entirely on economical Arm many-core processors [32].

However, these solutions are suboptimal for efficient CPU-based LLM serving due to not addressing the vastly different demands in the *prefill* and the *decode* phases of the workload, as identified by many distributed solutions [45, 46, 67].

In the *prefill* phase, the LLM model is executed on an input sequence to generate the first token and populate the key-value cache (KV cache). Since the procedure is computational intensive and the input sequence has variable length, an efficient tensor program that handles dynamic-shaped input is required. Existing solutions [10, 12, 25, 35, 41, 52] are either vendor-specific or hand-crafted, with limited adaptation to dynamic shapes. Automatic tensor program schedulers like TVM [7] generate shape-specific static tensor program templates, but may incur substantial auto-tuning costs due to their extensive search space of kernel implementations, especially when handling dynamic-shape tensor programs. To address this issue, existing dynamic shape compilers [59, 63, 68] often encode hardware primitives into the *computation slices*, also referred to as micro-kernels (MKs), that partially compute the result at compile time, and apply some *polymerization schemes* (how the MKs are assigned concurrently to computing resources) at runtime. This approach can significantly reduce the search overhead by encoding expert heuristics into the MKs. However, they either adopt the scale-up-and-out [68] method, (greedily expand the MK shapes for each cache level, such as the SRAM and the HBM in the GPU, and then partitioning them among available processing units), or the cost-model-based approach that utilize fix-sized MKs and leverage a cost model for their polymerization at runtime. Although larger MKs exhibit better efficiency, they reduce the parallelizability of the tensor program, which limits the optimization space for the polymerization scheme. Both approaches overlook this interplay, leading to suboptimal kernel performance.

In the *decode* phase, subsequent tokens are generated one at a time based on the existing KV cache. While not being computational intensive, this procedure requires a large number of read access to the model parameters and the KV cache. Modern many-core CPUs employ non-uniform memory access (NUMA) for higher

[†]Equal contribution.

aggregated computing power, which comes at the cost of memory latency caused by cache contention, thread synchronization, and remote memory access across NUMA nodes [33]. Current approaches mitigate memory contention through quantization or approximation techniques [50, 61], suffering degraded generation quality. There has been no discussion on active CPU core numbers and locations, while CPU possesses greater core autonomy through tools like OpenMP [44]. Although a reduced number of threads can decrease computation power and limit parallelization, it is more likely to alleviate memory bus contention during highly memory-bounded decode phase [6]. In addition, despite some attempts to advocate NUMA-aware thread scheduling [20, 28, 32] or evenly partition the model among NUMA nodes [26] to mitigate the cross-NUMA memory access overhead, they do not consider sub-structures beneath the NUMA level, such as the four-core cluster sharing a last-level cache (LLC) in EPYC 7H11 processors [1], which advocates for finer partition within a NUMA node.

Further, existing compilers typically require a deep understanding of their domain-specific language (e.g., TIR [17]), incurring difficulty in porting third-party hand-crafted kernels (e.g., attention [10, 18, 36]).

We propose Sandwich, a lightweight, hardware-centric LLM serving engine that separately addresses the challenges in prefill and decode phases with efficient generation of dynamic-shaped tensor programs and a streamlined automated tuning pipeline that solves both the model partition and core utilization problem. Sandwich generates MKs with different shapes and expands them with a fast-start-then-finetune approach by enumerating polymerization schemes and computation slices. Sandwich also parses and enumerates CPU topological information in a tree format, systematically exploring all core utilization plans regarding shared latent hardware structures. Trees are then transformed into LLM service configurations, including the core utilization of tensor programs and the partition plan of the model, among which the best configuration is selected with an efficient algorithm. We summarize our contributions as follows:

- We characterize the LLM workload on NUMA systems and identify shared resource contention as a bottleneck of decode phase performance. We also highlight the necessity of limiting active cores to a specific number and locations, adhering to a latent memory hierarchy in the NUMA system.

- We propose a streamlined approach of exploring core utilization plans under a modeled topology. With TopoTree, a mutable tree-based hardware abstraction representing processing units with leaf nodes and shared hardware resources with non-leaf nodes, we define two tree transformations: (1) group, which enumerates latent intermediate structures, and (2) remove, which alleviates potential memory bus bottlenecks. These transformations yield a search space that contains the optimal CPU service configuration, maximizing parallelism while effectively mitigating resource contention.

- We design a fast-start-then-finetune approach to generate dynamic-shape tensor programs with jointly optimized replicable computation slices and polymerization schemes. It reduces unnecessary kernel tuning steps and achieves superior kernel performance in the prefill step.

- We conduct extensive experiments with Sandwich using various chatbot traces on different CPU platforms (Xeon Gold 6151,

6230, Platinum 8272CL, EPYC 7H12, and Kunpeng 920). Sandwich achieves up to 3.40× shorter inference latencies and average 2.01× end-to-end serving speedup than the best existing solutions, and produces comparable kernel performance to TVM with three-order-of-magnitude less tuning cost.

2 Background

LLM serving. LLM serving is an autoregressive next-token prediction: generate each subsequent token according to the prompt and previously generated tokens, one at a time, and repeat this procedure until the end of the sequence is reached or a maximum number of tokens is exceeded.

The token generation consists of two phases. In the prefill phase, the entire user prompt is processed to generate the first token and the initial key-value (KV) cache, which makes it compute-bound. The variable length of the input sequence also calls for dynamic-shape tensor programs. The decode phase emits one token at a time based on the stored KV cache, which is the predominant phase in LLM serving [6] and memory-bound. Consequently, the application service level objectives (SLOs) of LLM limits the time to first token (TTFT), corresponding to the prefill latency, and the time per output token (TPOT), corresponding to the decode latency.

Model Partition. Existing CPU serving solutions [2, 20, 35] offer the option to partition the model across multiple processes. This is commonly known as tensor parallelism (TP) or model parallelism [51]. The assignment of processes to CPU cores is usually determined by their NUMA group and remains the same during the entire execution [2, 20, 35]. We use *service configuration* to refer to the combination of a model partition plan that distributes the model into processes and a core utilization plan that decides the core number and locations for each process.

Memory Hierarchy of a NUMA system. Modern CPUs are usually equipped with multi-level cache hierarchies that improve the performance of tasks with data-locality [1, 29]. Conventionally, level-one caches (L1 caches) are the fastest, smallest, and private to each CPU core. Last-level cache (LLC) are the slowest, largest, and shared by multiple CPU cores. In the context of a NUMA system, all the cache hierarchy fits under a single NUMA node. Tree-based abstractions of the memory hierarchy have been used to model the performance of such systems [16, 58]. Multiple core accessing shared data simultaneously might put pressure on shared resources such as memory controllers [11, 37].

Dynamic-shape Tensor Program Generation. Static-shape compilers [7] fail at this task because of their unacceptable time of tuning every input shape.

Dynamic-shape compilers construct tensor programs using *computation slices*, also known as micro-kernels (MK), which are single-threaded programs that cover certain tensor shapes, and *polymerization schemes*, which are schedules to place the computation slices onto parallel computation resources. They can be categorized into two approaches. Scale-up-and-out [68] is a bottom-up approach that gradually increases the size of the computation slice by repeating a MK along some dimension and selecting the scale-up dimension that yields the most performance gain through profiling. When the performance improvement saturates at a cache level, the computation slice is treated as a new MK and the process is

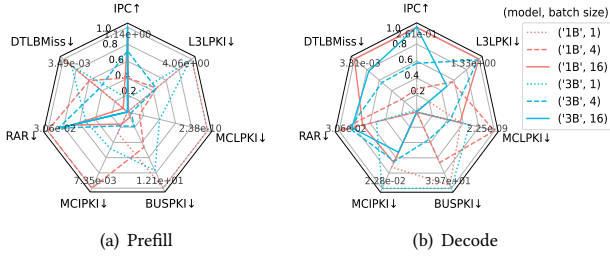


Figure 1: Prefill and decode workload characterization using different performance counters for single-sequence and batched serving of Llama3.2-1B and Llama3.2-3B.

repeated. Eventually, a computation slice is constructed for the LLC and it is replicated among all CPU cores. A cost-model-based method [59, 63] is a top-down approach that uses fixed-shape pre-compiled computational slices, whose polymerization schedules are determined at runtime by a cost model. Our observation shows that both approaches fail at providing the optimal tensor program.

3 Observations and Opportunities

3.1 Prefill-decode workload difference

Sec. 2 reveals that the prefill phase and the decode phase require substantially different algorithms for performance optimization. To identify workload characteristics of these phases on a many-core CPU, we adopt metrics proposed in [11, 47]: (1) Instructions Per Cycle (IPC): number of instructions per cycle; (2) Last-level Cache Loads Per Thousand Instructions (L3LPKI); (3) Data Transaction-Lookaside Buffer (TLB) Misses (DTLBMiss): ratio of dTLB misses that cause page-table walks, a process taking multiple memory accesses to translate virtual memory addresses to physical ones, to dTLB loads; (4) Remote Access Ratio (RAR): ratio of cross-NUMA remote memory accesses to total memory accesses; (5) Memory Controller Loads Per Thousand Instructions (MCLPKI); (6) Memory Controller Imbalance Per Thousand Instructions (MCIPKI): standard deviation of loads across all memory controllers (between different cache levels of a NUMA system); and (7) Bus Cycles Per Thousand Instructions (BUSPKI). We run BF16 Llama3.2-1B [14] and Llama3.2-3B [53] models on a system of two Intel Xeon Platinum 8275CL CPUs (each featuring 24 physical cores across two NUMA nodes), using vLLM [35]. We also partitioned the model evenly between the two NUMA nodes, as recommended [35]. Requests are sampled from the ShareGPT dataset [49] with batch sizes of 1, 4, and 16 (sequences).

Observation #1: Different characteristics of prefill and decode workloads. As Fig. 1 shows, the prefill phase has a higher IPC and lower BUSPKI. This indicates a compute-centric workload where memory accesses to shared cache are separated by computation tasks, exerting less pressure on the memory controller of the NUMA node. In contrast, the decode phase experiences lower IPC and significantly higher BUSPKI and MCLPKI. Therefore, the prefill phase requires more computational power, while the decode phase needs to avoid congestion at memory controllers. Existing CPU serving solutions [2, 20, 35] apply the same core utilization plan throughout the entire execution (Sec. 2), without taking care of

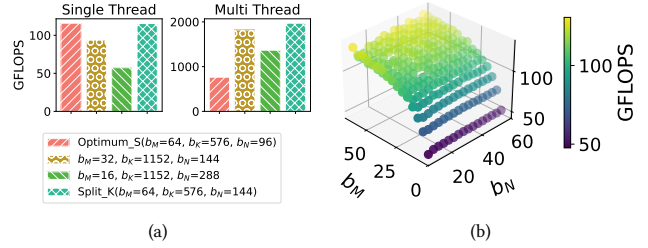


Figure 2: GEMM: (a) GFLOPS under different combinations of compute block and threading schemes; (b) Block size vs. GFLOPS when increasing b_M, b_N .

the more computation required by the prefill phase or the memory bandwidth needed by the decode phase.

Existing GPU serving solutions [46, 67] divide GPUs into prefill clusters and decode clusters. This is inapplicable to a NUMA system of CPUs due to the limited number of cores on CPUs: dividing the cores into prefill and decode clusters only reduces the capability of meeting the TTFT goal [39].

Opportunity: separate execution plans for prefill and decode phases. Our observation reveals that the prefill and decode phases put pressure on different components in the NUMA system, while CPU’s multi-threading model allows greater core autonomy compared to GPU’s single-program-multiple-data (SPMD) model. We propose to compute the prefill phase using a service configuration including all cores and a collection of kernel programs maximizing computational performance under each input shape. For the decode phase, we switch to another service configuration optimized specifically for the memory-bounded operations.

3.2 The prefill phase

As mentioned in 2, a major challenge in the prefill phase is generating dynamic-shape tensor programs. Existing LLM-serving solutions adopt vendor and hand-tuned kernels (e.g. Attention [10, 35], positional embedding [52], fused kernels). Kernel libraries such as XNNPack, Bolt [25], and oneDNN [41] provide manually written kernels that are efficient only in a certain range of input shapes [12]. Dynamic-shape compilers miss the optimal tensor program for the following reasons.

Observation #2: Computation slices and polymerization schemes require joint optimization. A larger computation slice may improve data locality on faster low-level caches, but it also limits the parallelizability of certain axes. This may under-utilize available CPU cores, or eliminate polymerization schemes promoting data locality on a higher cache level, depending on the input data orientation.

To verify this, we construct a two-level GEMM operation using the Basic Linear Algebra Subprograms (BLAS) structure [5], which consists of a macro-kernel and a micro-kernel, corresponding to per-core caches and vector registers in data-center CPUs [1, 29, 54], shaped by b_M, b_N, b_K and μ_M, μ_N, μ_K , respectively. For simplicity, we initialize $(\mu_M, \mu_N) = (4, 4)$ and $\mu_K = b_K$, and change b_M, b_N, b_K to maximize per-core cache utilization. We collect GFLOPS data for the GEMM operation with dimensions $(M, N, K) = (128, 1152, 2304)$ on a 2-NUMA system with two Xeon 6230 CPUs using 32 threads in

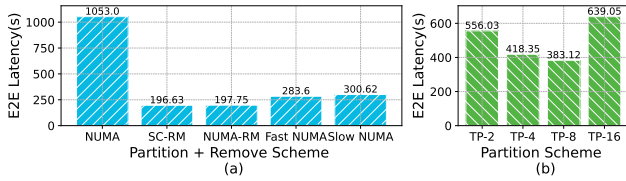


Figure 3: (a) Kunpeng: i) NUMA: using all the NUMA nodes; ii) SC-RM: removing one core from every 4 cores; iii) NUMA-RM: removing the same number of cores as SC-RM, but the last cores in each NUMA node; iv) Fast NUMA: using fast NUMA nodes only; v) Slow NUMA: using slow NUMA node; (b) AMD EPYC 7H21: comparison among different TP degrees.

total, varying the macro-kernel sizes, as shown in Fig. 2(a). Optimizing for maximum cache utilization, the scale-up-and-out method produces a computation slice of $(b_M, b_N, b_K) = (64, 96, 576)$ (Optimum_S), which achieves the best single-thread performance; however, it leaves only 24 threads for scale-out, failing to utilize 32 cores concurrently. Meanwhile, setting $(b_M, b_N, b_K) = (32, 144, 1152)$ is much better than $(b_M, b_N, b_K) = (16, 288, 1152)$, which, however, are regarded equivalent by the cost-model-based method [59]. In addition, the cost model cannot distinguish them from the K-split scheme on the reduction dimension [59], while $(b_M, b_N, b_K) = (64, 144, 576)$ yield the optimal performance.

Observation #3: Scale-up can be faster in the initial steps. Existing method [68] uses a constant step size to scale up a computation slice, while we observe an initial period when we can adopt a larger step. In Fig. 2(b), we benchmark GFLOPS of a GEMM with $(M, N, K) = (512, 768, 1024)$, using an MK size of $(\mu_m, \mu_n) = (4, 4)$. We scale up the block size along the M and N dimensions from $(4, 4)$ at a step size of 4, to generate different b_M and b_N . Increasing b_M , the GFLOPS grow initially rapidly but eventually converge to a similar growth rate with b_N . The advantage of scaling up the M dimension early is so significant that some decisions could be skipped.

Opportunity: Joint Optimization and Fast Start. The scale-up method can effectively generate high-performance single-thread computation slices while the cost-model-based approach provides polymerization maximizing parallel hardware utilization. We propose a joint-optimization method without compromising any side. In the scale-up process, inspired by momentum optimization [34] and TCP congestion control [30], we employ a *fast-start* strategy to rapidly expand the initial program and skip relatively simple early decisions. This is followed by a *finetune* adjustment stage, which enumerates possible polymerization schemes and uses finer steps to scale up the computation slices to uncover the optimal solution.

3.3 The decode phase

The decode phase consists of frequent memory accesses that could potentially saturate shared hardware resources such as memory controllers. Existing GPU serving solutions always perform computation on all GPU cores. We show that resource contention can be reduced by decreasing active CPU cores selectively with respect

to shared resources, which are sometimes opaque to the operating system or the user.

Observation #4: Numbers and physical locations of active cores impact performance. Following the hypothesis that the performance improvement is due to reduced competition of shared resources, we run the same serving experiments on a system with four Kunpeng-920 CPUs (Arm-based server CPUs) featuring 192 cores with 8 NUMA nodes in total, using a TP size of 8. We intentionally deactivate 6 cores from usage: either at the LLC Tag cluster level with one core among every four cores disabled, or one core per NUMA node disabled. Latencies differ across NUMA nodes in the system, making 4 NUMA nodes fast and the other 4 slow. We further experiment with a TP size of 4 to evaluate the end-to-end latency per request when using fast or slow NUMA nodes only. Fig. 3(a) demonstrates different performances of utilizing all cores and 4 core-reduction scenarios that all deactivate the same amount of cores following the strategies above. Notably, peak performance may be obtained by disabling cores with respect to the latent architectures, which are shared resources opaque to system utilities “Istopo”, e.g., deactivating one core per LLC Tag cluster, as shown in Fig. 5, on Kunpeng CPUs alleviates pressure on the shared LLC tag arrays, which holds information that translates data addresses in lower-level caches to corresponding ones in the LLC.

At the same time, improving data locality for lower-level caches within a NUMA node may also improve performance. As shown by Fig. 3(b), a TP size of 8 for a 2-NUMA EPYC 7H11 [1] system, where each CPU contains 64 cores and a total of 16 LLCs each shared by 4 cores, reduces data access across 4 groups of 4 LLCs under each NUMA node, alleviating the pressure to maintain cache coherence.

Opportunity: Optimizing core utilization and model partition according to the memory hierarchy Our findings emphasize the critical role of deliberate CPU core activation in reducing resource contention during LLM serving. Additionally, they reveal the advantages of exploiting spatial locality and hardware-aware model partitioning to achieve improved synergy in CPU-based LLM serving. To effectively capture latent shared structures (such as LLC Tag clusters), and to abstract away the black art of core selection and model partition, we propose a tree-based, streamlined methodology for LLM service configuration generation. Specially, we introduce the **TopoTree**, a mutable tree-based representation of all possible core utilization plans under a specific hierarchical shared memory system, coupled with two tree transformations, *group* and *remove*. By establishing a projection between each tree and a single LLM service configuration, these transformations ensures each model partition occupies only CPU cores under some latent shared structures, which improves data locality selectively.

4 Sandwich Overview

Sandwich consists of two main components as shown in Fig. 4, service configuration generation (S1) and kernel orchestration (S2) are ran offline. In the service configuration generation, Sandwich parses the CPU (NUMA) architecture using system tools and constructs the fundamental *TopoTree*, modeling the memory hierarchy using a tree. An exploration stage then enumerates all possible latent sub-structures between tree nodes, followed by a group transform to discover all core utilization plans with all cores activated for

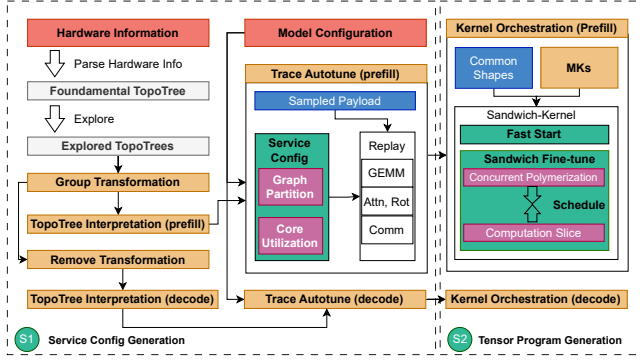


Figure 4: Compile-time workflow of Sandwich

prefill, and a remove transform to discover all core utilization plans with some cores removed for decode. Both results are given to TopoTree interpretation, where *sandwich-config* algorithm generates the spectrum of service configurations from a TopoTree. In the tensor program generation, *sandwich-kernel* algorithm generates a collection of computational slices and their polymerization plans for dynamic shapes required by the LLM model, separately for prefill and decode stage. Finally, the two service configurations and collections of tensor programs are used at runtime, for the prefill and decode phases respectively.

5 Service Configuration Generation

5.1 TopoTree Abstraction

TopoTree is a multi-level tree structure that represents core utilization plans under a NUMA system with a shared resource hierarchy. As illustrated in Fig. 5 ①, the *fundamental TopoTree* is constructed based on hardware information collected through system tools like “Istopo” [42]: the leaf nodes are the processing units (PUs) where actual computation takes place, encompassing both virtual and physical CPU cores; non-leaf nodes correspond to resources shared among descendant nodes, e.g., L3 cache for Physical Units (PUs) within the same Super Core Cluster (SCCL).

TopoTree is designed for the *automation* of tree generation and optimization. We facilitate the exploration of the latent shared structure by grouping tree nodes while mitigating the contention via strategic node removal. A *TopoTree* serves as a mapping between PUs and their associated shared resource hierarchy. It can be further utilized to represent a family of service configurations, i.e., delineating how to utilize the hardware resources including the process number, core distribution, and memory hierarchy association (e.g., NUMA information). Consequently, the service configuration search space is isomorphic to the domain of viable *TopoTree* variants.

5.2 Tree Transformation

To fully explore applicable *TopoTrees* (service configurations) from a *fundamental TopoTree*, we design group and remove transformations on the tree. We have two observations regarding the service configuration and the *TopoTree*:

► **Symmetric and Tileable:** To constrain the search space, contemporary intra-op parallelism predominantly adheres to the SPMD

paradigm [13, 35, 66]. SPMD assumes homogeneous compute capacity across cores, with instructions distributed uniformly. Such an assumption generally holds for CPUs, barring heterogeneous architectures like big.LITTLE [3]. Consequently, this paradigm corresponds to a *TopoTree* structure characterized by isomorphic subtrees. Additionally, since nodes in TopoTree are organized by clustering, this ensures the number of PUs reachable by any of its direct children is equal.

► **Latent Shared Structure:** System tools like “Istopo” do not fully expose the shared structure (mainly CPU cache coherent interconnect and L3-Tags). As shown in Fig. 5, for a system consisting of four Kunpeng920 CPUs [55], 1scpu has information that 24 cores belong to the same NUMA (L3 cache), but lacks the structure information that every CCL (4 cores) shares an L3-Tag, which might incur contention for I/O operations.

With these observations in mind, we propose the two transformations to explore the *TopoTree* (different service configurations). Given a *TopoTree* with $L(d)$ nodes at level d , $\text{group}(n, t, d)$ inserts $L(d)/n$ new nodes that group $n \geq 2$ nodes each with a stride t at a specified depth d , thereby forming a new level within the *TopoTree*. $\text{remove}(n, d)$ eliminates n right-most children of each node at the specified depth $d - 1$. Starting from the *fundamental TopoTree*, Sandwich first uses group to explore the latent shared structure to enumerate descendant TopoTrees with different possible shared structures. Then the remove transformation is applied to these explored TopoTrees (which now incorporate new node grouping relationships) to mitigate potential shared resource contention at various hierarchical levels. In Fig. 5, ① gives the *fundamental TopoTree* obtained by parsing the visible hardware structure using system tools. Then in ②, some group transformations aggregate every four cores, forming a new hierarchical level of the TopoTree that identifies the latent L3-Tag shared structure. Subsequently in ③, a remove transformation eliminates specific cores, mitigating contention on the newly discovered L3-Tag structure in the explored TopoTree. Here remove can be applied to L3-Tag/CCL nodes to reduce L3 cache contention as well.

Sandwich systematically enumerates possible group and subsequent remove transformations until no further candidates are available. Since group transformations preserve parent-child relationships in the tree, their order is inconsequential. Each descendant tree resulting from remove represents a new spectrum of service configurations. Consequently, we collect intermediate *TopoTrees* generated by remove operations, while disregarding those produced solely by group transformations. Leveraging the ‘Symmetric and Tileable’ assumption, we apply transformations concurrently to nodes at the same hierarchical levels with the following complexity. **Complexity of Group Transformations.** Let $\mathcal{S}(n)$ represent the number of all possible *TopoTrees* among n CPU cores, $\text{all_children}(s)$ represents all underlying PUs of node s , and $\text{cpu_id}(c)$ represents the id of PU c provided by the manufacturer. We make the following assumptions:

ASSUMPTION 1. In a *TopoTree*:

- A.1 (Symmetric) every subgraph is symmetric;
- A.2 (Tiled by Stride) for an arbitrary subgraph with set S of direct children of the subgraph, there exists a stride $t \in \mathbb{N}_{>0}$ and an element $s_0 \in S$ such that for any subgraph $s' \in S$ and for all cores

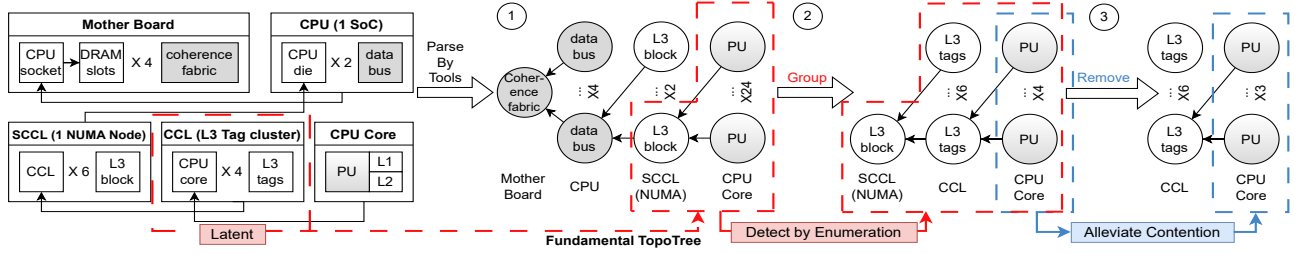


Figure 5: Example TopoTree and its transformations on Kunpeng920.

$c' \in \text{all_children}(s')$, there exists a core $c \in \text{all_children}(s_0)$ satisfying $\text{cpu_id}(c') = qt + \text{cpu_id}(c)$, where $q \in \mathbb{N}$;

A.3 (Power of Two): $n = 2^x$ for $x \in \mathbb{N}_{>0}$.

A.1 and A.2 hold under our observations. A.3 applies to most data center CPUs with a large number of cores.

$O(S(n))$ represents the upper-bound complexity of possible TopoTrees explored by group transformations. Let $F(n, h)$ denote the number of all possible ways to partition n subgraphs into clusters of size h . By our assumption and Stirling's approximation [22], the following proposition outlines the complexity.

PROPOSITION 1 (COMPLEXITY OF GROUP TRANSFORMATIONS).

$$O(S(n)) = \begin{cases} O\left(\frac{n^n}{(n-1)!}\right) \approx O(e^n), & \text{Under A.1, A.2} \\ O\left(\frac{n^{\frac{\log_2 n}{2}}}{(n-1)!}\right), & \text{Under A.1, A.2 and A.3} \end{cases} \quad (1)$$

The complexity is acceptable because: 1) the maximum number of cores in a subgraph visible by system tools is usually much smaller, $n_s \ll n$; 2) for non-datacenter CPUs, n is quite small. For data center CPUs, the complexity in (1) is limited to factorial growth in the denominator and the slower (exponential) growth in the numerator; the complexity converges to $O(1)$ as n increases. In our experimental setup, TopoTree search using *group* transformations can be completed within minutes (1.18 - 600s).

Complexity of Remove Transformations. Given a TopoTree after group transformations, the complexity of remove transformations among all possible groups of nodes is given by:

PROPOSITION 2 (COMPLEXITY OF REMOVE TRANSFORMATIONS). *The complexity of remove on a grouped tree is $O(n^2)$.*

Detailed proofs can be found in the appendix. The complexity of *remove* becomes vast as the number of cores increases. Fortunately, we observe opportunities to efficiently reduce the remove transformation search space:

1) *Equilivant TopoTrees*: Different remove transformation paths can lead to common intermediate tree representations. Inspired by the Merkle tree used in blockchain [31], we generate a header hash for each tree based on its structure and node features. A *TopoTree* is only considered for a subsequent remove transformation if it is new.

2) *Transformation Tree*: While remove transformations initially enhance performance by mitigating resource contention, they may eventually degrade efficiency due to reduced computation parallelism. If a descendant tree from a remove transformation yields no performance improvement over its parents, its further descendants

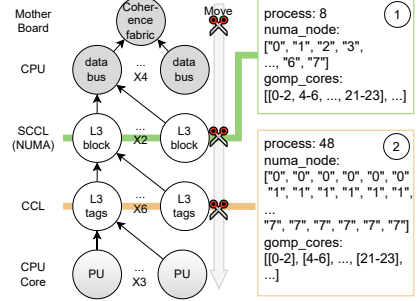


Figure 6: Example TopoTree Interpretation

are pruned. Successive remove transformations on a parent tree constitute a transformation tree, as illustrated in Fig. 4 ("tree of transformation"). At depth d of the transformation tree, remove candidates are determined by the number of nodes at $d - 1$. We employ topological sorting to traverse the transformation tree from the root. If any node is discardable, all its descendants are eliminated.

5.3 TopoTree to Service Configuration

CPU cores can be grouped or partitioned at either the **thread** or the **process** level. As a result, different model parallelization strategies can be executed on the same *TopoTree*. As illustrated in Fig. 6, 144 cores can be configured in two ways: ① 8 processes (corresponding to TP=8 in our scenario) with 16 cores each, or ② 48 processes with 3 cores each

To enumerate candidate service configurations from a TopoTree, we propose the **sandwich-config** algorithm. This algorithm starts at the tree's root and progresses level-wise, applying a horizontal cross-section (as depicted in Fig. 6). Nodes intersecting this cross-section determine the process count and their associated memory hierarchy (e.g., NUMA), while the subtrees beneath these nodes delineate core spatial locality and utilization strategies.

The complexity of the **sandwich-config** algorithm is constrained by the TopoTree height, which in turn depends on the number of cores. With a maximum height of $\log_2(k)$, where k is the number of cores, the algorithm's complexity is $O(\log_2(k))$. In practice, this value is typically less than 10. We further propose several practical heuristics to speed up service configuration generation.

1) *Equivalent Configuration*: Hashing and eliminating the same configurations met during the algorithm procedure.

2) *Operator Limitations*: Certain operators restrict the possible tensor-parallel degrees. For example, the TP degree of attention must be divisible by the number of KV-heads and query heads, which puts a limit to the largest TP.

3) *Early Stopping*: We further enable early stopping, using a patience score to halt when consecutive non-optimal results are reached. We group service configurations with the same process number and NUMA information, and introduce early stopping within each group. If early stopped, all configurations in that process group are discarded.

We determine the optimal service configurations in terms of end-to-end latency through latency simulation based on sampled token generation traces. It is noteworthy that kernel performance can significantly impact service configuration outcomes due to its direct influence on latencies. However, simultaneously identifying the best service configuration and tensor schedule would lead to very high search complexity. For efficiency, when identifying the best service configurations, we adopt a default tensor schedule generated by a cost model-based polymerization method [63]. Then we provide top-k best service configurations among all TopoTrees for subsequent kernel orchestration. In our experiments, this approach has demonstrated both performance superiority and efficiency with $k = 10$.

6 Tensor Program Generation

Given a model partition plan, the prefill shapes are known except for the input sequence length. This allows us to generate tensor programs for all possible shapes in the inference process, considering input sequence length up to the maximum allowed by the model. We design a **sandwich-kernel** approach to generate tensor schedules for dynamic shapes under a specific service configuration. Besides using the fast-start-and-finetune strategy proposed in Sec. 3.2, Sandwich also utilizes the similarity of the LLM prefill shapes to advocate a sliding window technique and tensor program reuse to reduce tuning time.

Micro-Kernel Generation. Sandwich generates MKs of size $\mu_M \times \mu_N \times K$, where μ_M and μ_N rows of data along the reduction dimension K are loaded, multiplied, and accumulated using SIMD registers. Similar to Roller [68], Sandwich generates MKs tailored to align with CPU processing units, particularly focusing on avoiding register spilling, which can degrade performance. As modern CPUs are typically equipped with 32 vector registers, Sandwich enumerates potential MK candidates utilizing up to 32 registers. The size of reduction dimension b_K is also aligned with the cacheline size, which is the maximum number of bytes loaded into a cache simultaneously.

Fast-start and finetune. Similar to [59, 63, 68], Sandwich constructs a tensor program by scaling up computation slices along the cache hierarchy with every MK from the previous step. To efficiently utilize the initial steps and simultaneously search for concurrent thread polymerization and replicable computation slices, we propose a two-phase approach: a fast initial search followed by fine-tuning.

1) *Fast Start*: Like TCP [30], we expand the shape of a computation slice with an exponentially growing step of $2^{t_D} \times \text{tile size}$, where t_D is the accumulated expansion step size on dimension

D . The performance (GFLOPS) of the growing kernel is collected by profiling at each step. If any expansion on a dimension D fails to provide performance gains or degrades performance, the size of the computation slice is rolled back to the previous step along this dimension. To avoid reducing the search space for polymerization schemes as mentioned in Sec. 3.2, we stop expanding a dimension if doing so limits its parallelizability. For example, for $(M, N, K) = (128, 64, 64)$ and $\text{nthread} = 2$, the maximum size of the computational slice should be limited to $(64, 32, 32)$.

2) *Finetune*: After fast start, we enumerate thread polymerization schemes utilizing all CPU cores available to the tensor program. Under each scheme, we grow the computational slice along the dimension that provides the most efficiency, until the best computation slice is found. Finally, we compare the efficiency of the result tensor programs under every polymerization scheme and MK to choose the best one.

Micro-kernel sliding window & tensor schedule reuse. Since many input shapes in the prefill workload shares the same sizes for dimensions except the one representing sequence length, we process such input shapes in groups and order them by the size of the input dimension, starting from 1. We propose two optimizations to speed up the tuning:

1) *Sliding window*: For a large enough sequence length, the MK yielding the optimal tensor program is always the one that exploits data reuse the most with vector registers, but when the input sequence length is relatively small, the input shape is skewed and requires a diverse set of candidate MKs. We create a sliding window of size σ . For the first σ shapes, we use all MKs as candidates; for the following shapes, we only consider the σ -last chosen MKs. This helps us identify and prioritize the most effective MKs for larger token sizes while sustaining a diverse selection of MKs for small token sizes. In our experiments, a σ of 16 yields a good balance between scheduling overhead and tensor schedule quality.

2) *Tensor Schedule Reuse*: As the token size continues to grow, the polymerization scheme and the shape of the computation slice tend to stabilize. This stability occurs because the shape becomes less skinny, and large enough to obtain optimal computation slices without reducing the search space of polymerization. We set an empirical early-stopping criterion for tensor schedule searches. When the new optimal slice's difference is within a threshold of the previous average, the slice will be fixed for the following shapes. The same policy applies to threads. In addition, we cache the searched schedules to avoid repetition across different shape groups. With the optimal slice and polymerization, Sandwich can easily generate a schedule for the unseen larger shape by dividing the input shape with the polymerization plan and repeating the computation slice on each division.

7 Dual-IR and Runtime Implementation

Sandwich is implemented with 14,400 lines of Python code and 6,700 lines of C++ code. It is fully integrated with vLLM [35], incorporating optimizations such as continuous batching [60], and can be directly invoked using vLLM commands. Kernel optimizations like positional embedding [52], FlashAttention [10], and PagedAttention [35] have been parsed to IR and incorporated into our codebase, ensuring seamless integration and support across multiple devices.

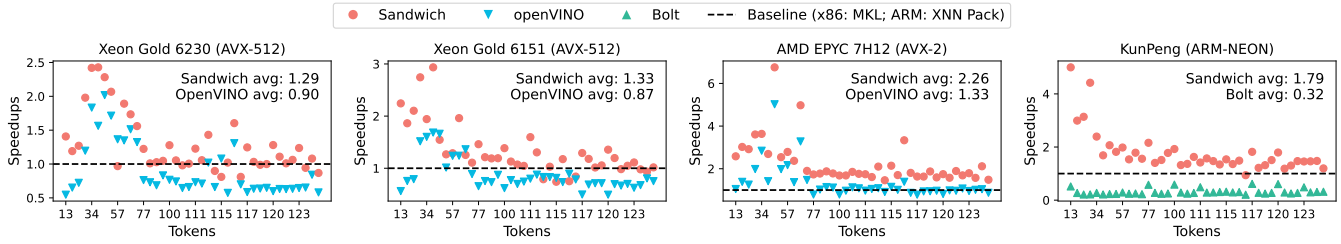


Figure 7: Comparison of kernel execution speed-up among Sandwich and vendor solutions.

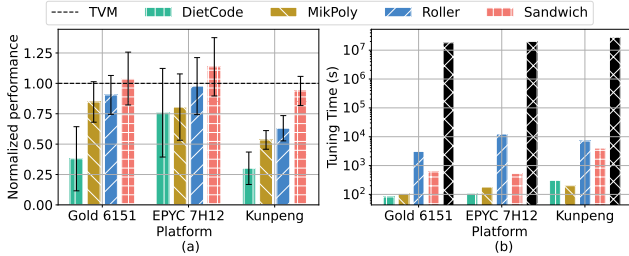


Figure 8: Kernel generation comparison among Sandwich and other compilers: (a) Normalized kernel performance; (b) Tuning time.

7.1 Dual-IR

Specialized hand-crafted kernels, such as attention kernels, typically necessitate labor-intensive reimplementations on a target hardware platform and compiler DSL. To expose and tune customized key parameters while ensuring portability from existing tensor programs, Sandwich kernel compiler adopts a dual-level IR architecture: a low-level IR with a syntax resembling the low-level programming language used for LLM kernels (e.g., C++) for easy adoption, and another high-level IR with Python-like syntax for abstracting SIMD instructions and easier insertion of key parameters (in the case of our GEMM tensor schedule, encompassing μ_M, μ_K in MKs). Complex hand-crafted tensor programs are first parsed to our low-level IR, and then to the Python-like IR for tuning.

7.2 Rank-Shifted Share Memory Communication

We implement efficient inter-process communication using shared memory (SHM). The master process obtains a file descriptor and distributes it to worker processes, which then cache and map it for shared data access. During all-reduce operations, workers wait for the master to complete data copying, accumulate their data in shared memory, and copy the result back to their local memory. Despite its efficiency for data sharing [26], this approach faces challenges in handling concurrent accesses and variable data sizes.

We propose a rank-shifted adaptive SHM communication approach, inspired by the geometric circular shift method from [48]. This approach assigns a unique rank-based shift to each process, creating a circular writing pattern that enables concurrent execution without waiting. We dynamically adapt the shared memory block size, ensuring it exceeds the cache-line size to avoid false sharing [4].

8 Evaluation

8.1 Experimental Settings

Platform. We evaluate Sandwich across various NUMA systems. For x86 architectures, we use (i) 2x Intel(R) Xeon(R) Gold 6151 CPU (2 NUMA nodes) with 18 physical cores (PC) / 36 virtual cores (VC) each [56], (ii) 2x Xeon Gold 6230 CPU with 20 PC / 40 VC each (2 NUMA nodes) [29], (iii) 2x Xeon Platinum 8272CL CPU with 24 PC / 48 VC each (2 NUMA nodes) [9], and (iv) 2x AMD EPYC 7H12 with 64 PC / 128 VC each (2 NUMA nodes). The prior two CPUs have AVX-512 vector extension. The latter one has AVX-2 vector extension. For aarch64 (ARM), we assess 4x Kunpeng 920 CPUs with 8 NUMA nodes, 192 PCs, and NEON instructions[54].

Model Precision. We employ BF16 for experiments on AVX-512 CPUs, and FP32 for those on AVX-2 and Kunpeng platforms. Notably, since TVM does not support BF16 tuning on CPUs, we utilize FP32 for kernel experiments for a clear comparison across different CPU platforms and compilers.

Model and workload. We run the Llama series [53], a prominent family of LLMs. For dynamic-shape benchmarks, we create a payload generator to produce all possible shapes of the operator for a model, given the maximum sequence length and model configuration, such as hidden size, intermediate size, KV, and query head numbers. The input sequence lengths are sampled within a specified range to generate the test payloads, and we explicitly use cores on a single NUMA node for these experiments to avoid interference. We tune all possible shapes with maximal sequence length seq_{max} for compiler comparison.

For serving, we evaluate both single sequence and batched serving. We generate serving workloads based on the chatbot dataset ShareGPT and LMSys-Chat-1M [64]. For single sequence serving, we sample 90 test requests from the datasets and feed them into the serving system sequentially. For batched serving, request arrival times are generated using a Poisson distribution with varying request rates [35, 67].

Metrics. For dynamic-shape benchmarks, we measure operator latency speed-ups (with performance normalized to that of TVM) and tuning time. For serving, we adopt SLO attainment as our primary metric. Additionally, we measure (1) the average token generation throughput during single-sequence serving, and (2) Goodput for batched serving, defined as the maximum request rate that can be sustained while meeting the SLO attainment goal. Consistent with the previous study [67], we set the SLO attainment goal to 90% (i.e., P90). The SLO parameters are empirically determined as described in Sec. 8.3.

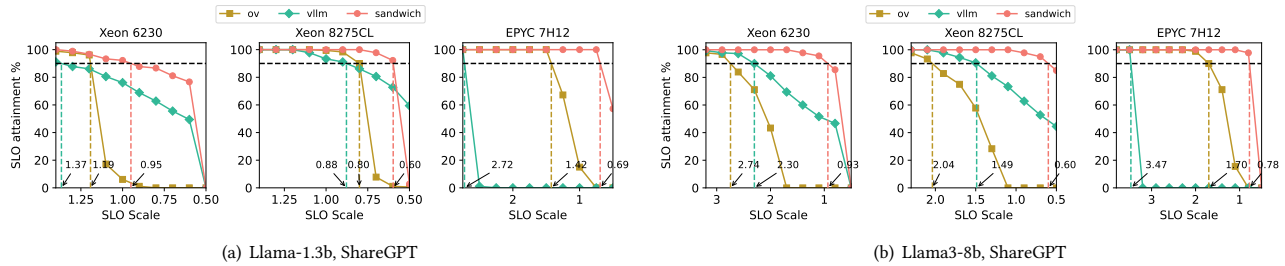


Figure 9: Comparison of SLO attainment percentage under different SLO scales.

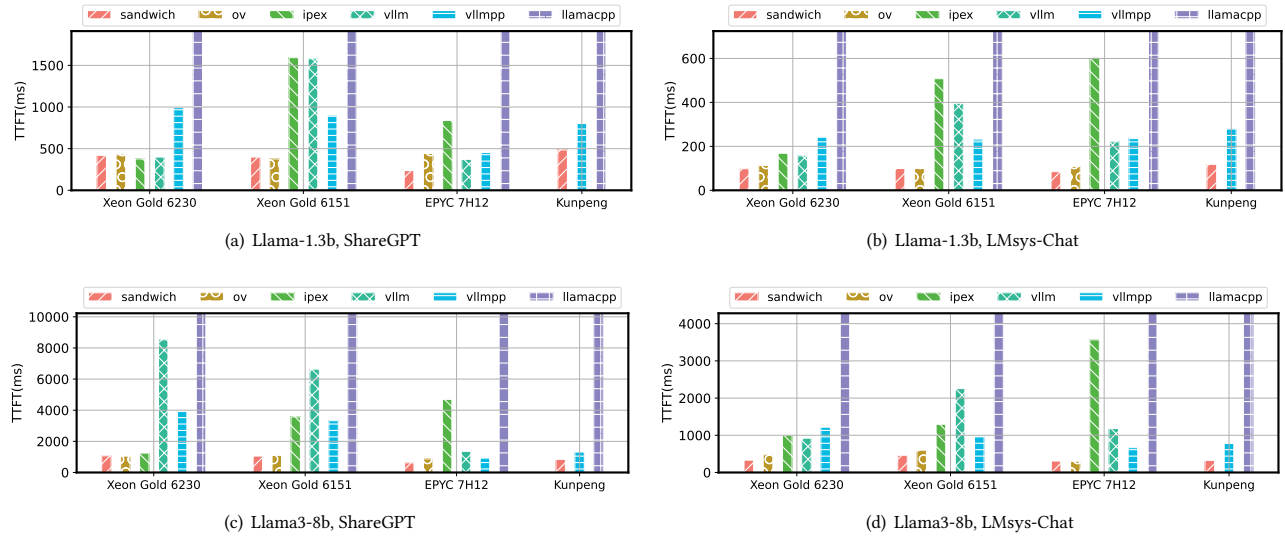


Figure 10: Comparison of TTFT in single sequence serving.

Baselines. The dynamic-shape solutions that we compare with are: (1) standard GEMM operators from DNN frameworks and vendor-specific solutions, including MKL-DNN [27] and OpenVINO [28] for x86, and Bolt [25] and Torch with XNNPACK [57] on ARM SoC; (2) compiler solutions such as TVM Ansor [65], and dynamic-shape solutions DietCode, Roller, and MikPoly [59, 63, 68]. Since these solutions are originally designed for GPUs, we reimplement them for CPUs by translating their scheduling policies. We provide them the same MK candidates used by Sandwich, and only differ from them in polymerization. AutoTVM [8] does not provide an official code for CPU linear ops, thus not included.

We also compare Sandwich with various serving solutions.

- Hardware-specific vendor solutions: (1) intel-extendon-for-pytorch (ipex) [50], and (2) OpenVINO (ov) [28].
- GPU-serving solutions: (3) vLLM [35] with its default CPU backend and no model partition; (4) vLLM++ (vllmpp) [67], a vLLM version that enumerates TP strategies for optimal performance, where NUMA node and cores are partitioned evenly (to distinguish it from vLLM, we set vllmpp with a minimum TP size of 2).
- SOTA open-source solution (5) llama.cpp [20].

For Sandwich, we obtain $topk = 10$ service configurations and identify the best performance among them. We do not compare with xFasterTransformer [26] as it is mainly optimized for advanced

instructions with at least AVX512-bf16, and offers poor support to our CPU platforms.

8.2 Dynamic-Shape Benchmark

In this section, we compare the performance of Sandwich-generated kernels against baseline methods on commonly used shapes. Specifically, we conduct a case study on GEMM, which is the primary computational operator in LLMs.

Vendors. We first compare with vendor solutions for x86 and ARM architectures, namely MKL and XNNPack. Fig. 7 illustrates the speedups of the Sandwich kernel relative to the vendor and third-party libraries. The x-axis specifies the token size, each representing a set of all possible GEMM operations conducted during serving (e.g., QKV, FFN) in a Llama-1.3b model. For each kernel, we perform a warmup of 5 times and repeat the measurement 100 times to obtain average results.

Sandwich achieves $1.27 - 4.02\times$ speedup compared to the baselines, and outperforms other solutions (e.g., OpenVINO and Bolt) in most cases. Notably, Sandwich demonstrates more efficiency for kernels with smaller M -size ($M < 64$); when the token size is larger (token size > 100), the speedup over different solutions tends to decrease. We attribute this to the fact that as M increases, the kernel becomes less skinny, allowing vendor solutions to perform well.

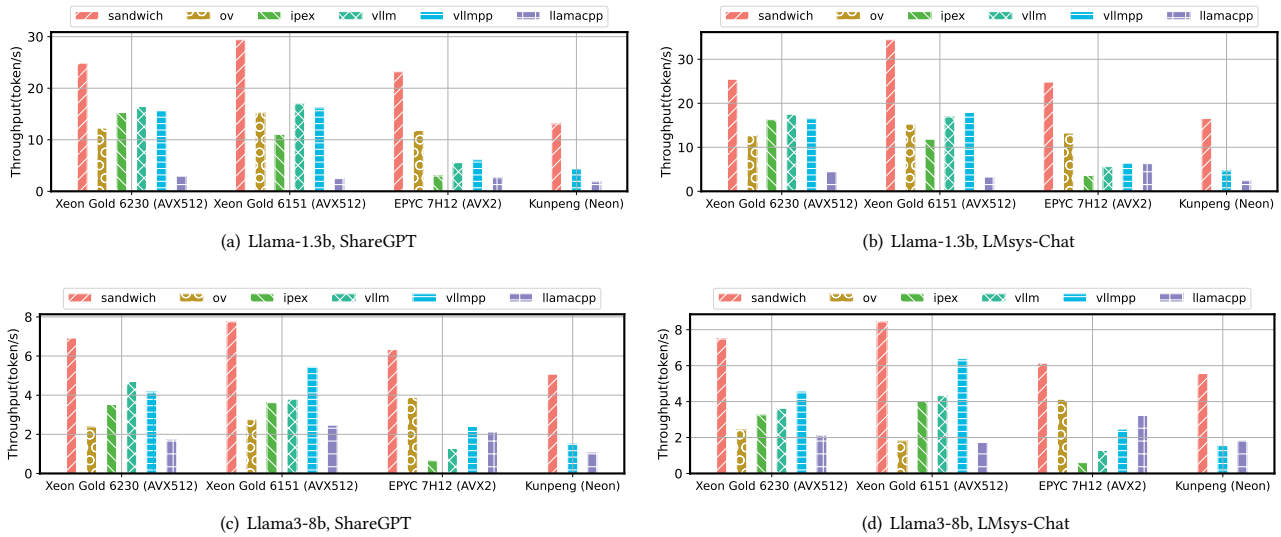


Figure 11: Comparison of output token generation throughput for single sequence serving.

Compilers. We further compare kernel program performance normalized against TVM and tuning time over Gold 6151, EPYC 7H12, and Kunpeng platforms. For AutoTVM [8], we set the number of tuning trials to 800, as recommended in their official documentation, and allow early stopping. Due to its extended tuning time, we sample only 20 shapes to tune with TVM. We range the token size in $[1, seq_{max}]$, where seq_{max} is specified in the model configuration in the tuning process. Fig. 8(a) shows that Sandwich’s kernel achieves better or comparable performance relative to the TVM tuner, while Fig. 8(b) reveals that Sandwich requires less than 90% of the tuning time, as compared to TVM. Sandwich is faster than Roller in terms of tuning time due to its quick start and effective tensor-schedule reuse. Cost-model-based methods, such as DietCode and MikPoly, are extremely fast in tuning but fail to provide competitive kernel performance. Sandwich outperforms all other compilers because it jointly optimizes both concurrent polymerization and parallelizable schemes.

8.3 Serving Benchmark

SLOs. Since there exist no available SLO settings for these models as far as what we know, we set the SLOs empirically. In single sequence serving, time-to-first-token (TTFT) SLO is set to 2200ms and time-per-output-token (TPOT) SLO to 70ms for the 1.3B model; TTFT is set to 8000ms and TPOT to 240ms for the 8B model. In batch serving, P90 of TTFTs should be no larger than 200ms and P90 of TPOTs 100ms for the 160M model; P90 TTFT is set to 2000 ms and P90 TPOT to 280 ms for the 1.3B model. We also introduce *SLO scale* to vary the SLO latencies. A lower SLO scale corresponds to more stringent latency requirements.

Single Sequence Serving. We conduct extensive serving experiments under twomodel sizes (1.3B, and 8B) on four platforms. As shown in Fig. 9, Sandwich can sustain 90% SLO attainment with up to 3.40 \times , and 4.45 \times more stringent SLOs, compared to OpenVINO and vLLM. As for token generation throughput and TTFT, Sandwich achieves an average 2.01 \times higher throughput, shown

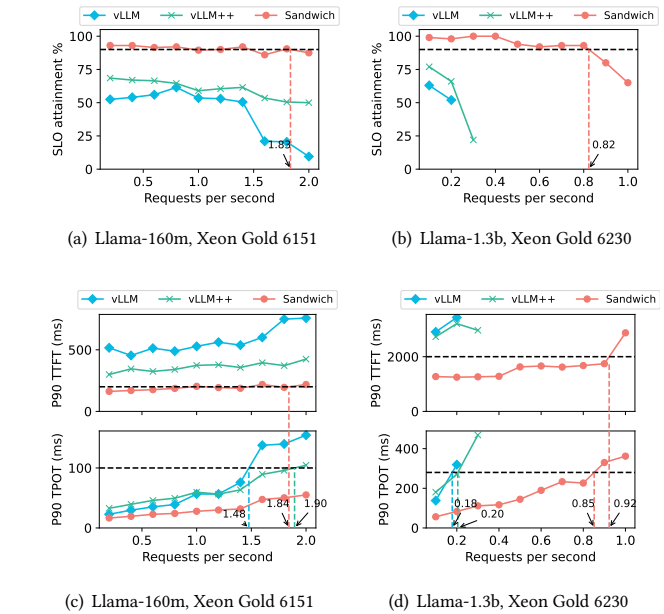


Figure 12: SLO and Goodput comparison for batched serving.

in Fig. 11, and similar TTFT, shown in Fig. 10, across all sample cases compared to the best vendor and open-source solutions. The tuning time of service configurations used in the experiments of Sandwich ranges from 78s to 3279s, with an average of 1309s. The kernel tuning time from $[1, seq_{max}]$ ranges from 2022s to 23115s, averaging 10155s.

Batch Serving. We evaluate batch serving on 160M and 1.3B Llama models. Since vLLM supports only BF16 and AVX-512 inference, we conduct experiments on the Xeon 6151 and 6230 processors. As we gradually increase the request rate, P90 TPOT and TTFT results are collected. Fig. 12 shows that Sandwich can handle a higher request rate (1.84 and 0.92 requests per second) while meeting the TPOT

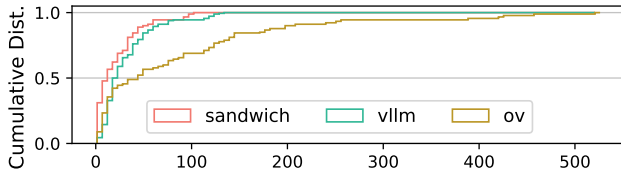


Figure 13: Request latency distribution for Llama3-8B, batch size=1, ShareGPT input, on Xeon 6230.

Optimizaton	BS=1	BS=8
vLLM	4.09	2.35
+ communication op	13.46	3.66
+ service config	14.90	5.40
+ kernel tuning	17.54	8.16
+ split k	17.09	8.78

Table 1: Ablation study on different optimizations used in Sandwich. Serving Llama 3.2-3B on Xeon 8272CL. The values are throughput (token/s).

k	tuning time (s)	throughput (token/s)
5	4,716.86	15.46
10	9,609.13	15.58
15	13,443.91	16.19
20	16,497.87	16.42

Table 2: Ablation study on different values of k in selecting the top- k service configurations. Serving single sequences on Llama 1.3b, EPYC 7H12.

ρ	tuning time (s)	TTFT (ms)	throughput (token/s)
5	490.99	645.07	15.38
10	377.92	627.14	14.86
15	972.93	621.76	15.51
20	832.30	590.22	15.48

Table 3: Ablation study on different values of hyperparameter ρ used in Sandwich. Serving single sequences on Llama 1.3b, EPYC 7H12.

and TTFT requirements. In contrast, the original vLLM consistently fails to satisfy the TTFT requirement.

Latency Distribution Fig. 13 is a CDF plot of the inference latency distribution of requests made to Llama3-8B on Xeon 6320 with batch size 1. Sandwich’s latency distribution shifts significantly toward lower values, indicating that our optimizations greatly reduce inference latency and result in a higher proportion of requests experiencing shorter delays.

8.4 Ablation Study

We conduct an ablation study to demonstrate the latency reduction and throughput gains achieved by different techniques in Sandwich. Table 1 shows that our communication optimization, service

configuration tuning, and kernel tuning each improve token generation throughput by varying degrees under different batch sizes. Notably, split- k (parallelizing the reduction dimension) does not benefit single-sequence serving, but it improves small-batch (BS=8) throughput. The variation arises from the presence of search space pruning. Employing split- k needs careful tuning. Table 2 shows that as more top- k service configurations from trace autotune are considered in the tensor program generation, higher throughputs are achieved in the LLM serving at the cost of extra tuning time. Table 3 shows an ablation study of the sliding window size ρ in the tensor program generation. A larger ρ allows consideration of more MKs before the computation slice expands to a large enough size where the MK is stable. A larger ρ yields better prefill performance and also shorter tuning time in some cases, since profiling an inefficient computation slice takes more time.

9 Related Works

Tree-based Hardware Abstraction. Tree-based abstractions [16, 21, 58] have been used for describing memory hierarchies of shared memory systems, such that nodes represent memory buffers (e.g., DRAM, caches) shared by its children. Such abstractions are usually used for describing task assignments and memory allocations. Sandwich introduces TopoTree, a mutable memory hierarchy representation, to accelerate the search for latent shared resources and suitable service configurations.

Parallel Tensor Program Optimizations. The MK-based approach to optimize dynamic-shaped linear algebra programs could be traced back to the HPC era [19, 23, 38]. Manual implementation and experiments have concluded that computing MKs to introduce data locality is essential for optimal performance on systems with a hierarchical memory, and the size of Mks depend on the input shape. Sandwich particularly handles the skewed input shapes (with a dynamic relatively small sequence length dimension and limited parallel potential) that appeared in the LLM prefill phase.

Tensor Program Compilers. Static-shaped tensor program compilers like AutoTVM/Ansor [8, 65] utilize an evolutionary algorithm to search a huge optimization space. Dynamic-shaped compilers take the scale-up-and-out approach, proposed by Roller [68] or the cost-model-based approach, proposed by DietCode [63] and MikPoly [59]. Sandwich surpasses the static-shaped approach in tuning speed because of a sophisticated search space and exceeds dynamic-shaped approaches in performance because of its joint consideration of computation slice and polymerization scheme.

10 Conclusion

This paper introduces Sandwich, a compilation framework for efficient CPU-based LLM-serving. Sandwich constructs a hardware-centric search space to optimize CPU core utilization and model partition granularity, enhancing LLM serving performance. Using fast-start and fine-tuning, the kernels generated by Sandwich outperform vendor kernels and other compiler solutions, matching static compiler performance with order-of-magnitude less tuning time. Our extensive experiments demonstrate that Sandwich achieves significant throughput gains, substantial Goodput improvement and can be used to serve under tighter latency SLO setups.

References

- [1] AMD. n.d.. Server Processor Specifications.
- [2] Reza Yazdani Aminabadi, Samyag Rajbhandari, Ammar Ahmad Awan, Cheng Li, Du Li, Elton Zheng, Olatunji Ruwase, Shaden Smith, Minjia Zhang, Jeff Rasley, and Yuxiong He. 2022. DeepSpeed-inference: enabling efficient inference of transformer models at unprecedented scale. In *Proceedings of the International Conference on High Performance Computing, Networking, Storage and Analysis (SC '22)*. IEEE Press, Dallas, Texas, Article 46, 15 pages.
- [3] ARM. 2025. Arm big.LITTLE. <https://www.arm.com/technologies/big-little>
- [4] Emery D. Berger, Kathryn S. McKinley, Robert D. Blumofe, and Paul R. Wilson. 2000. Hoard: a scalable memory allocator for multithreaded applications. In *Proceedings of the Ninth International Conference on Architectural Support for Programming Languages and Operating Systems*. Association for Computing Machinery, New York, NY, USA, 117–128.
- [5] L Susan Blackford, Antoine Petit, Roldan Pozo, Karin Remington, R Clint Whaley, James Demmel, Jack Dongarra, Iain Duff, Sven Hammarling, Greg Henry, et al. 2002. An updated set of basic linear algebra subprograms (BLAS). *ACM Trans. Math. Software* 28, 2 (2002), 135–151.
- [6] Lequn Chen, Zihao Ye, Yongji Wu, Danyang Zhuo, Luis Ceze, and Arvind Krishnamurthy. 2023. Punica: Multi-Tenant LoRA Serving.
- [7] Tianqi Chen, Thierry Moreau, Ziheng Jiang, Lianmin Zheng, Eddie Yan, Haichen Shen, Meghan Cowan, Leyuan Wang, Yuwei Hu, Luis Ceze, Carlos Guestrin, and Arvind Krishnamurthy. 2018. TVM: An Automated End-to-End Optimizing Compiler for Deep Learning. In *13th USENIX Symposium on Operating Systems Design and Implementation (OSDI 18)*. USENIX Association, USA, 579–594.
- [8] Tianqi Chen, Lianmin Zheng, Eddie Yan, Ziheng Jiang, Thierry Moreau, Luis Ceze, Carlos Guestrin, and Arvind Krishnamurthy. 2019. Learning to Optimize Tensor Programs.
- [9] CPU-World. 2024. Intel Xeon Platinum 8272CL specifications.
- [10] Tri Dao, Daniel Y. Fu, Stefano Ermon, Atri Rudra, and Christopher Ré. 2022. FlashAttention: Fast and Memory-Efficient Exact Attention with IO-Awareness.
- [11] Mohammad Dashti, Alexandra Fedorova, Justin Funston, Fabien Gaud, Renaud Lachaize, Baptiste Lepers, Vivien Quema, and Mark Roth. 2013. Traffic management: a holistic approach to memory placement on NUMA systems. In *Proceedings of the Eighteenth International Conference on Architectural Support for Programming Languages and Operating Systems (Houston, Texas, USA) (ASPLOS '13)*. Association for Computing Machinery, New York, NY, USA, 381–394.
- [12] Yaoyao Ding, Cody Hao Yu, Bojian Zheng, Yizhi Liu, Yida Wang, and Gennady Pekhimenko. 2023. Hidet: Task-Mapping Programming Paradigm for Deep Learning Tensor Programs. In *Proceedings of the 28th ACM International Conference on Architectural Support for Programming Languages and Operating Systems, Volume 2 (Vancouver, BC, Canada) (ASPLOS 2023)*. Association for Computing Machinery, New York, NY, USA, 370–384.
- [13] Jianguo Du, Jinhui Wei, Jiazhi Jiang, Shenggan Cheng, Dan Huang, Zhiguang Chen, and Yutong Lu. 2024. Liger: Interleaving Intra- and Inter-Operator Parallelism for Distributed Large Model Inference. In *Proceedings of the 29th ACM SIGPLAN Annual Symposium on Principles and Practice of Parallel Programming (Edinburgh, United Kingdom) (PPoPP '24)*. Association for Computing Machinery, New York, NY, USA, 42–54.
- [14] Abhimanyu Dubey, Abhinav Jauhri, Abhinav Pandey, Abhishek Kadian, Ahmad Al-Dahle, Aiesha Letman, Akhil Mathur, Alan Schelten, Amy Yang, Angela Fan, et al. 2024. The llama 3 herd of models. arXiv:2407.21783 [cs.AI]
- [15] Jiarui Fang, Yang Yu, Chengduo Zhao, and Jie Zhou. 2021. TurboTransformers: an efficient GPU serving system for transformer models. In *Proceedings of the 26th ACM SIGPLAN Symposium on Principles and Practice of Parallel Programming (Virtual Event, Republic of Korea) (PPoPP '21)*. Association for Computing Machinery, New York, NY, USA, 389–402.
- [16] Kayvon Fatahalian, Timothy J. Knight, Mike Houston, Mattan Erez, Daniel Reiter Horn, Larkhoon Leem, Ji Young Park, Manman Ren, Alex Aiken, William J. Dally, and Pat Hanrahan. 2006. Sequoia: Programming the Memory Hierarchy. In *SC '06: Proceedings of the 2006 ACM/IEEE Conference on Supercomputing*. Association for Computing Machinery, New York, NY, USA, 4–4.
- [17] Siyuan Feng, Bohan Hou, Hongyi Jin, Wuwei Lin, Junru Shao, Ruihang Lai, Zihao Ye, Lianmin Zheng, Cody Hao Yu, Yong Yu, and Tianqi Chen. 2022. TensorIR: An Abstraction for Automatic Tensorized Program Optimization.
- [18] Xiao Fu, Weiling Yang, Dezun Dong, and Xing Su. 2024. Optimizing Attention by Exploiting Data Reuse on ARM Multi-core CPUs. In *Proceedings of the 38th ACM International Conference on Supercomputing (Kyoto, Japan) (ICS '24)*. Association for Computing Machinery, New York, NY, USA, 137–149. <https://doi.org/10.1145/3650200.3656620>
- [19] Kyle A. Gallivan, William Jalby, Ulrike Meier, and Ahmed H. Sameh. 1988. Impact of Hierarchical Memory Systems On Linear Algebra Algorithm Design. *International Journal of High Performance Computing Applications* 2 (1988), 12 – 48. <https://api.semanticscholar.org/CorpusID:62189292>
- [20] Georgi Gerganov and contributors. 2023. llama.cpp: LLaMA inference in C/C++.
- [21] Millad Ghane, Sunita Chandrasekaran, and Margaret S. Cheung. 2019. Gecko: Hierarchical Distributed View of Heterogeneous Shared Memory Architectures. In *Proceedings of the 10th International Workshop on Programming Models and Applications for Multicores and Manycores (Washington, DC, USA) (PMAM '19)*. Association for Computing Machinery, New York, NY, USA, 21–30.
- [22] Ronald L. Graham, Donald E. Knuth, and Oren Patashnik. 1994. *Concrete Mathematics: A Foundation for Computer Science*. Addison-Wesley Longman Publishing Co., Inc., USA.
- [23] John A. Gunnels, Greg M. Henry, and Robert A. Geijn. 2001. A Family of High-Performance Matrix Multiplication Algorithms. In *International Conference on Conceptual Structures*. <https://api.semanticscholar.org/CorpusID:442764>
- [24] Qinghao Hu, Zhisheng Ye, Zerui Wang, Guoteng Wang, Meng Zhang, Qiaoling Chen, Peng Sun, Dahua Lin, Xiaolin Wang, Yingwei Luo, Yonggang Wen, and Tianwei Zhang. 2024. Characterization of Large Language Model Development in the Datacenter. In *21st USENIX Symposium on Networked Systems Design and Implementation (NSDI 24)*. USENIX Association, Santa Clara, CA, 709–729.
- [25] Huawei Noah. Year. Bolt: A Deep Learning Library with High Performance and Heterogeneous Flexibility. <https://github.com/huawei-noah/bolt>. Accessed on Date.
- [26] Intel. 2023. xFasterTransformer.
- [27] Intel Corporation. 2024. Intel Math Kernel Library.
- [28] Intel Corporation. 2024. Intel OpenVINO Toolkit.
- [29] Intel Corporation. n.d.. Intel® Xeon® Gold 6230 Processor (27.5M Cache, 2.10 GHz) - Specifications.
- [30] V. Jacobson. 1988. Congestion avoidance and control. In *Symposium Proceedings on Communications Architectures and Protocols (Stanford, California, USA) (SIGCOMM '88)*. Association for Computing Machinery, New York, NY, USA, 314–329.
- [31] Kiseok Jeon, Junghee Lee, Bumsoo Kim, and James J. Kim. 2023. Hardware Accelerated Reusable Merkle Tree Generation for Bitcoin Blockchain Headers. *IEEE Computer Architecture Letters* 22, 2 (2023), 69–72.
- [32] Jiazhi Jiang, Jianguo Du, Dan Huang, Dongsheng Li, Jiang Zheng, and Yutong Lu. 2023. Characterizing and Optimizing Transformer Inference on ARM Many-core Processor. In *Proceedings of the 51st International Conference on Parallel Processing (Bordeaux, France) (ICPP '22)*. Association for Computing Machinery, New York, NY, USA, Article 20, 11 pages.
- [33] Jiazhi Jiang, Jianguo Du, Dan Huang, Dongsheng Li, Jiang Zheng, and Yutong Lu. 2023. Characterizing and Optimizing Transformer Inference on ARM Many-core Processor. In *Proceedings of the 51st International Conference on Parallel Processing (Bordeaux, France) (ICPP '22)*. Association for Computing Machinery, New York, NY, USA, Article 20, 11 pages.
- [34] Diederik P. Kingma and Jimmy Ba. 2017. Adam: A Method for Stochastic Optimization.
- [35] Woosuk Kwon, Zhuohan Li, Siyuan Zhuang, Ying Sheng, Lianmin Zheng, Cody Hao Yu, Joseph Gonzalez, Hao Zhang, and Ion Stoica. 2023. Efficient Memory Management for Large Language Model Serving with PagedAttention. In *Proceedings of the 29th Symposium on Operating Systems Principles (Koblenz, Germany) (SOSP '23)*. Association for Computing Machinery, New York, NY, USA, 611–626.
- [36] Hao Liu, Matei Zaharia, and Pieter Abbeel. 2023. Ring Attention with Blockwise Transformers for Near-Infinite Context.
- [37] Zoltan Majo and Thomas R. Gross. 2011. Memory system performance in a NUMA multicore multiprocessor. In *Proceedings of the 4th Annual International Conference on Systems and Storage*. Association for Computing Machinery, New York, NY, USA, 10 pages. <https://doi.org/10.1145/1987816.1987832>
- [38] Kafil K. Mathur and S. Lennart Johnsson. 1994. Multiplication of Matrices of Arbitrary Shape on a Data Parallel Computer. *Parallel Comput.* 20 (1994), 919–951. <https://api.semanticscholar.org/CorpusID:16487869>
- [39] Seonjin Na, Geonhwa Jeong, Byung Hoon Ahn, Jeffrey Young, Tushar Krishna, and Hyesoon Kim. 2024. Understanding Performance Implications of LLM Inference on CPUs. In *2024 IEEE International Symposium on Workload Characterization (IISWC)*. IEEE, 169–180.
- [40] NVIDIA. 2023. FasterTransformer.
- [41] oneDNN Contributors. 2024. oneAPI Deep Neural Network Library (oneDNN). <https://github.com/oneapi-src/oneDNN>
- [42] Open MPI. 2023. hwloc. <https://github.com/open-mpi/hwloc>.
- [43] OpenAI. 2023. ChatGPT: Optimizing Language Models for Dialogue.
- [44] OpenMP Architecture Review Board. 2008. OpenMP Application Program Interface Version 3.0. <http://www.openmp.org/mp-documents/spec30.pdf>
- [45] Archit Patke, Dharmath Reddy, Saurabh Jha, Haoran Qiu, Christian Pinto, Chandra Narayanaswami, Zbigniew Kalbarczyk, and Ravishankar Iyer. 2024. Queue Management for SLO-Oriented Large Language Model Serving. In *Proceedings of the 2024 ACM Symposium on Cloud Computing (Redmond, WA, USA) (SoCC '24)*. Association for Computing Machinery, New York, NY, USA, 18–35. <https://doi.org/10.1145/3698038.3698523>
- [46] Ruoyu Qin, Zheming Li, Weiran He, Mingxing Zhang, Yongwei Wu, Weimin Zhang, and Xinran Xu. 2024. Mooncake: A KVCache-centric Disaggregated Architecture for LLM Serving. *ArXiv abs/2407.00079* (2024).

- [47] Hongliang Qu and Zhibin Yu. 2024. WASP: Workload-Aware Self-Replicating Page-Tables for NUMA Servers. In *Proceedings of the 29th ACM International Conference on Architectural Support for Programming Languages and Operating Systems, Volume 2 (ASPLOS '24)*. Association for Computing Machinery, New York, NY, USA, 1233–1249.
- [48] Sudarsanan Rajasekaran, Manya Ghobadi, and Aditya Akella. 2023. CASSINI: Network-Aware Job Scheduling in Machine Learning Clusters. arXiv:2308.00852 [cs.NI]
- [49] RyokoAI. 2021. ShareGPT52K.
- [50] Haihao Shen, Hanwen Chang, Bo Dong, Yu Luo, and Hengyu Meng. 2023. Efficient LLM Inference on CPUs. arXiv:2311.00502 [cs.LG]
- [51] Mohammad Shoeybi, Mostofa Patwary, Raul Puri, Patrick LeGresley, Jared Casper, and Bryan Catanzaro. 2019. Megatron-LM: Training Multi-Billion Parameter Language Models Using Model Parallelism. *ArXiv abs/1909.08053* (2019).
- [52] Jianlin Su, Yu Lu, Shengfeng Pan, Ahmed Murtadha, Bo Wen, and Yunfeng Liu. 2023. RoFormer: Enhanced Transformer with Rotary Position Embedding.
- [53] Hugo Touvron, Thibaut Lavril, Gautier Izacard, Xavier Martinet, Marie-Anne Lachaux, Timothée Lacroix, Baptiste Rozière, Naman Goyal, Eric Hambro, Faisal Azhar, Aurelien Rodriguez, Armand Joulin, Edouard Grave, and Guillaume Lample. 2023. LLaMA: Open and Efficient Foundation Language Models. arXiv:2302.13971 [cs.CL]
- [54] WikiChip. n.d.. Kunpeng 920-4826 - HiSilicon. <https://en.wikichip.org/wiki/hisilicon/kunpeng/920-4826>.
- [55] WikiChip. n.d.. TaiShan v110 - Microarchitectures - HiSilicon. https://en.wikichip.org/wiki/hisilicon/microarchitectures/taishan_v110. Accessed on July 25, 2025.
- [56] Wikipedia contributors. 2024. List of Intel Xeon processors (Skylake-based) – Wikipedia, The Free Encyclopedia.
- [57] XNNPack Contributors. 2024. XNNPack.
- [58] Yonghong Yan, Jisheng Zhao, Yi Guo, and Vivek Sarkar. 2009. Hierarchical place trees: a portable abstraction for task parallelism and data movement. In *Proceedings of the 22nd International Conference on Languages and Compilers for Parallel Computing (Newark, DE) (LCPC'09)*. Springer-Verlag, Berlin, Heidelberg, 172–187.
- [59] Feng Yu, Guangli Li, Jiacheng Zhao, Huimin Cui, Xiaobing Feng, and Jingling Xue. 2024. Optimizing Dynamic-Shape Neural Networks on Accelerators via On-the-Fly Micro-Kernel Polymerization. In *Proceedings of the 29th ACM International Conference on Architectural Support for Programming Languages and Operating Systems, Volume 2 (La Jolla, CA, USA) (ASPLOS '24)*. Association for Computing Machinery, New York, NY, USA, 797–812.
- [60] Gyeong-In Yu, Joo Seong Jeong, Geon-Woo Kim, Soojeong Kim, and Byung-Gon Chun. 2022. Orca: A Distributed Serving System for Transformer-Based Generative Models. In *16th USENIX Symposium on Operating Systems Design and Implementation (OSDI 22)*. USENIX Association, Carlsbad, CA, 521–538.
- [61] Tianyi Zhang, Jonah Wonkyu Yi, Bowen Yao, Zhaozhuo Xu, and Anshumali Shrivastava. 2024. NoMAD-Attention: Efficient LLM Inference on CPUs Through Multiply-add-free Attention. arXiv:2403.01273 [cs.LG]
- [62] Juntao Zhao, Borui Wan, Yanghua Peng, Haibin Lin, and Chuan Wu. 2024. LLM-PQ: Serving LLM on Heterogeneous Clusters with Phase-Aware Partition and Adaptive Quantization.
- [63] Bojian Zheng, Ziheng Jiang, Cody Hao Yu, Haichen Shen, Joshua Fromm, Yizhi Liu, Yida Wang, Luis Ceze, Tianqi Chen, and Gennady Pekhimenko. 2022. DietCode: Automatic Optimization for Dynamic Tensor Programs. In *Proceedings of Machine Learning and Systems*, Vol. 4. Conference on Machine Learning and Systems, USA, 848–863.
- [64] Lianmin Zheng, Wei-Lin Chiang, Ying Sheng, Tianle Li, Siyuan Zhuang, Zhanghao Wu, Yonghao Zhuang, Zhuohan Li, Zi Lin, Eric P. Xing, Joseph E. Gonzalez, Ion Stoica, and Hao Zhang. 2024. LMSYS-Chat-1M: A Large-Scale Real-World LLM Conversation Dataset. arXiv:2309.11998 [cs.CL]
- [65] Lianmin Zheng, Chengfan Jia, Minmin Sun, Zhao Wu, Cody Hao Yu, Ameer Haj-Ali, Yida Wang, Jun Yang, Danyang Zhuo, Koushik Sen, Joseph E. Gonzalez, and Ion Stoica. 2020. Ansor: generating high-performance tensor programs for deep learning. In *Proceedings of the 14th USENIX Conference on Operating Systems Design and Implementation (OSDI'20)*. USENIX Association, USA, Article 49, 17 pages.
- [66] Lianmin Zheng, Zhuohan Li, Hao Zhang, Yonghao Zhuang, Zhifeng Chen, Yanping Huang, Yida Wang, Yuanzhong Xu, Danyang Zhuo, Eric P. Xing, Joseph E. Gonzalez, and Ion Stoica. 2022. Alpa: Automating Inter- and Intra-Operator Parallelism for Distributed Deep Learning. In *16th USENIX Symposium on Operating Systems Design and Implementation (OSDI 22)*. USENIX Association, Carlsbad, CA, 559–578.
- [67] Yinmin Zhong, Shengyu Liu, Junda Chen, Jianbo Hu, Yibo Zhu, Xuanzhe Liu, Xin Jin, and Hao Zhang. 2024. DistServe: Disaggregating Prefill and Decoding for Goodput-optimized Large Language Model Serving.
- [68] Hongyu Zhu, Ruofan Wu, Yijia Diao, Shanbin Ke, Haoyu Li, Chen Zhang, Jilong Xue, Lingxiao Ma, Yuqing Xia, Wei Cui, Fan Yang, Mao Yang, Lidong Zhou, Asaf Cidon, and Gennady Pekhimenko. 2022. ROLLER: Fast and Efficient Tensor Compilation for Deep Learning. In *16th USENIX Symposium on Operating Systems*

Design and Implementation (OSDI 22). USENIX Association, Carlsbad, CA, 233–248.

A Proof of the complexity

Our goal is to find $O(S(n))$, the upper bound for our search space. Suppose $F(n, k)$ gives the number of all possible ways to partition n subgraphs into groups of size k , satisfying our requirements. Now we could define S inductively.

$$S(1) = 1 \quad (2)$$

$$S(n) = \sum_{k \in [2..n]} S\left(\frac{n}{k}\right) \cdot F(n, k) \quad (3)$$

Suppose $f(n, k, t)$ gives the number of all possible ways to partition n subgraphs into groups of size k , which could tile the original subgraph with a stride of t . Now we define F as

$$F(n, k) = \sum_{t \in [1.. \lfloor \frac{n}{k} \rfloor]} f(n, k, t)$$

Suppose we have a function $f(n, k, t)$ that gives the number of possible grouping for n cpus with groups of size k that could tile n using a stride of t . We have

$$f(n, k, t) \leq 1$$

Finally, we have

$$O(S(n)) = O\left(\sum_{k \in [1..n]} S\left(\frac{n}{k}\right) \cdot \sum_{t \in [1.. \lfloor \frac{n}{k} \rfloor]} 1\right) \quad (4)$$

$$= O\left(\left(\sum_{t \in [1..n]} t\right) \cdot \left(S\left(\frac{n}{2}\right) + S\left(\frac{n}{3}\right) + \dots + S\left(\frac{n}{n}\right)\right)\right) \quad (5)$$

$$= O\left(n \cdot \left(1 + \frac{n}{2}\right) \cdot \left(S\left(\frac{n}{3}\right) + \dots + S\left(\frac{n}{n-1}\right) + S(1)\right)\right) \quad (6)$$

$$= O\left(n \cdot \left(1 + \frac{n}{2}\right) \cdot \left(1 + \frac{n}{3}\right) \cdot \dots \cdot \left(1 + \frac{n}{n-1}\right) \cdot 1\right) \quad (7)$$

$$= O\left(\frac{n^n}{(n-1)!}\right) \quad (8)$$

A.1 Proof of the Remove Complexity

We analyze the complexity of the remove transformation in our search space, denoted as $O(S_r(n))$. Let $S(n)$ represent the maximum number of operations needed for a transformation involving n elements, which is characterized by recursive partitioning of the set. We express this relationship as follows:

$$\begin{aligned} S(n) &= \max_{k_0 \in [2, \dots, n]} \left((k_0 - 1) \times S\left(\frac{n}{k_0}\right) \right), \\ S\left(\frac{n}{k}\right) &= \max_{k_1 \in [2, \dots, \frac{n}{k}]} \left((k_1 - 1) \times S\left(\frac{n}{k \times k_1}\right) \right), \\ &\vdots \end{aligned} \quad (9)$$

To derive the upper bound, we examine the recursive relationship under the assumption that each division of the set maximizes the number of operations, which occurs when each partition is approximately equal in size. This assumption simplifies the analysis by focusing on the largest contributor to the complexity in each recursive step.

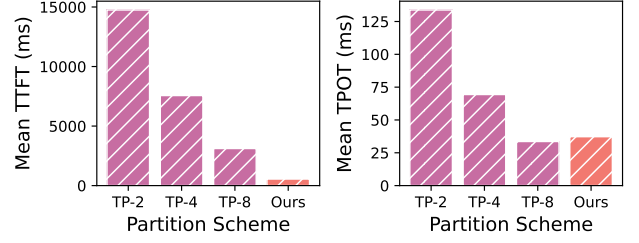


Figure 14: The mean TTFT and TPOT of xFasterTransformers serving Llama-1.3b under different partition schemes compared to our solution.

Consider the following cases for the recursive layering, denoted by L :

Case $L = 2$: The worst-case scenario occurs when the set is divided into \sqrt{n} groups of \sqrt{n} each, resulting in n operations. Case $L = 3$: Extending the argument, if the next layer also divides each group into $\sqrt{n/k}$, the complexity for this layer becomes $\frac{n}{k} \times k = n$, and the optimal choice for k remains \sqrt{n} . Generalizing from these observations, the recursive division continues, reducing the size of the problem in each layer by a factor that is a power of 2 (i.e., $n^{1/2}, n^{1/4}, \dots, n^{1/2^k}$). Summing over these contributions, the overall complexity can be expressed as:

$$O(S_r(n)) = n \times n^{1/2} \times n^{1/4} \times \dots \times n^{1/2^k}. \quad (10)$$

Each step in the recursion exponentially decreases the size of the problem, and the total complexity converges to n^2 , since the sum of the exponents in the product approaches 2:

$$1 + \frac{1}{2} + \frac{1}{4} + \dots + \frac{1}{2^k} \rightarrow 2 \quad \text{as } k \rightarrow \infty. \quad (11)$$

Thus, we conclude that the complexity of the remove transformation in our search space is $O(n^2)$.

B Other Results

We present a comparison with xFasterTransformer [26] in BF16 on Xeon Gold 6230. As illustrated in Fig. 14, Sandwich achieves substantial improvements in TTFT while maintaining compatible TPOT results, demonstrating its robust performance.

cpu	model	dtype	dataset	graph tune time (s)	kernel tune time (s)
Xeon Gold 6230	Felladrin/Llama-160M-Chat-v1	bfloat16	shapegpt	1212	7092
Xeon Gold 6230	Felladrin/Llama-160M-Chat-v1	bfloat16	lmsys-chat-1m	632	8673
Xeon Gold 6230	princeton-nlp/Sheared-LLaMA-1.3B	bfloat16	shapegpt	1106	7352
Xeon Gold 6230	princeton-nlp/Sheared-LLaMA-1.3B	bfloat16	lmsys-chat-1m	682	6032
Xeon Gold 6230	meta-llama/Meta-Llama-3-8B	bfloat16	shapegpt	2797	7544
Xeon Gold 6230	meta-llama/Meta-Llama-3-8B	bfloat16	lmsys-chat-1m	1389	12747
Xeon Gold 6151	Felladrin/Llama-160M-Chat-v1	bfloat16	shapegpt	496	9218
Xeon Gold 6151	Felladrin/Llama-160M-Chat-v1	bfloat16	lmsys-chat-1m	728	8142
Xeon Gold 6151	princeton-nlp/Sheared-LLaMA-1.3B	bfloat16	shapegpt	1098	13680
Xeon Gold 6151	princeton-nlp/Sheared-LLaMA-1.3B	bfloat16	lmsys-chat-1m	142	14237
Xeon Gold 6151	meta-llama/Meta-Llama-3-8B	bfloat16	shapegpt	3109	18168
Xeon Gold 6151	meta-llama/Meta-Llama-3-8B	bfloat16	lmsys-chat-1m	1202	16422
EPYC 7H12	Felladrin/Llama-160M-Chat-v1	float32	shapegpt	1915	2023
EPYC 7H12	Felladrin/Llama-160M-Chat-v1	float32	lmsys-chat-1m	1439	2717
EPYC 7H12	princeton-nlp/Sheared-LLaMA-1.3B	float32	shapegpt	1629	10540
EPYC 7H12	princeton-nlp/Sheared-LLaMA-1.3B	float32	lmsys-chat-1m	2157	4755
EPYC 7H12	meta-llama/Meta-Llama-3-8B	float32	shapegpt	2664	7912
EPYC 7H12	meta-llama/Meta-Llama-3-8B	float32	lmsys-chat-1m	1788	11843
Kunpeng 920	Felladrin/Llama-160M-Chat-v1	float32	shapegpt	262	3279
Kunpeng 920	Felladrin/Llama-160M-Chat-v1	float32	lmsys-chat-1m	79	4004
Kunpeng 920	princeton-nlp/Sheared-LLaMA-1.3B	float32	shapegpt	638	11410
Kunpeng 920	princeton-nlp/Sheared-LLaMA-1.3B	float32	lmsys-chat-1m	303	13386
Kunpeng 920	meta-llama/Meta-Llama-3-8B	float32	shapegpt	3280	19446
Kunpeng 920	meta-llama/Meta-Llama-3-8B	float32	lmsys-chat-1m	679	23115

Table 4: Tuning costs of Sandwich under different scenario